Japanese Journal of Applied Physics
Vol. 47, No. 1, 2008, pp. 764–767

Characteristics and Optical Properties of Ni Nanograins Reduced on TiO_2 Film

Hong-Hsin HUANG*, Hung-Peng CHANG[1], Fang-Hsing WANG[1], Yuan-Shing LIU, Moo-Chin WANG[2], and Ding-Fwu LII

Department of Electrical Engineering, Cheng Shiu University, 840 Cheng Ching Rd., Niaosong, Kaohsiung 83347, Taiwan
[1]*Department of Electrical Engineering and Graduate Institute of Optoelectronic Engineering, National Chung Hsing University, 250 Kuo Kuang Rd., Taichung 402, Taiwan*
[2]*Faculty of Fragrance and Cosmetics, Kaohsiung Medical University, 100 Shi-Chuan 1st Rd., Kaohsiung 80708, Taiwan*

(Received July 12, 2007; accepted October 4, 2007; published online January 22, 2008)

NiO/TiO_2 films with various NiO film thicknesses ranging from 10 to 320 nm were deposited on silicon and glass substrates by e-beam evaporation at 200 °C, and then annealed in H_2 atmosphere at 500 °C for 1 h in order to reduce the NiO film to Ni grains on the TiO_2 film. The structures of titanium oxide, NiO, and Ni/TiO_2 were determined by X-ray diffraction (XRD) analysis, and the morphology of the Ni/TiO_2 films was observed by scanning probe microscopy. The ultraviolet–visible (UV–vis) transmittance and vis absorption of the Ni/TiO_2 films were measured by UV–vis spectrophotometry. The results showed that an amorphous titanium oxide was obtained as deposited at 200 °C and that the structure change to the anatase phase after 500 °C annealing. As deposited, crystalline NiO films with XRD patterns similar to that of powder were obtained; however, diffraction peaks of (111) and (200) Ni appeared after annealing in H_2 atmosphere. Ni nanograins, coarsened grains, and films were obtained on the TiO_2 films when the NiO film with a thickness from 10 to 320 nm was reduced in H_2 atmosphere at 500 °C. The transmittance of the Ni/TiO_2 films decreased with an increase in Ni particle size. The vis absorption measurement showed that the peak shifted toward a shorter wavelength with a decrease in Ni particle size.
[DOI: 10.1143/JJAP.47.764]

KEYWORDS: Ni nanoparticle, visible-light absorption shift, transmittance, e-beam evaporation, morphology

1. Introduction

Titanium dioxide (TiO_2) films have beneficial physical and chemical properties and is one of the most important materials in optical, electronic, and chemical fields. It is used as an anti- and high-reflection coating, and as capacitor, solar cell, photocatalytic device,[1,2] and hydrophilic materials. New trends in reducing the size of microelectronic devices have enforced the use of high-permittivity oxides to fabricate metal–oxide–semiconductor field-effect transistor (MOSFET) structures with thicker oxides.[3] Titanium oxide, zirconium oxide, and hafnium oxides are of immediate interest owing to their high-permittivity factor and compatibility with silicon technology.[4–6] TiO_2 is generally considered to be the best semiconductor photocatalyst available for photocatalysis (PC) at present. Of possible greater significance are the recent findings of Fujishima *et al.*[7,8] that some semiconductors also exhibit a photoinduced superhydrophilic effect (PSH), i.e., they are rendered more wettable by water after exposure to ultra-band gap irradiation and that this process is reversible, albeit slow, in the dark.

Metal-support interactions can affect both catalyst activity and stability.[9] The techniques of metal-doped TiO_2 photocatalyst preparation, thermal treatment, and doping limitation, as well as doped titania properties and photoactivity were reviewed.[10] Anpo *et al.*[11] reported that visible light absorption is found in $Cr–TiO_2$ films by ion implanting and the order of the effectiveness in the redshift was found to be V > Cr > Mn > Fe > Ni ions. Such a shift allows the metal ion-implanted titanium oxide to use solar light more efficiently and effectively, at up to 20–30%. In the other case, the Cr-ion doped catalyst showed no shift in absorption band but a new absorption shoulder at aproximately 420 nm. The modified method of placing metal on TiO should affect the absorption of visible light.

A Ni/TiO catalyst was prepared by Yan *et al.*[12] for the partial oxidation of the methane reaction (POM) and it showed high activity and long-term stability in the CO-reforming reaction. Yan *et al.* reported that CH_4 is efficiently converted to CO and H via an oxidation mechanism when Ni/TiO is reduced, and pulse reaction studies provide evidence that the oxidation state of nickel controls the methane activation mechanism and product distribution. Titania-supported nickel catalysts are more active in CO hydrogenations than silica- or alumina-supported catalysts.[13] Two groups of catalyst have been used for methane activation to generate syngas: Ni-based catalysts[14] and noble-based catalysts.[15] The high-cost and limited availability of noble metals highlights the need to develop Ni-based catalysts, which can exhibit stability for extended periods.

Titanium oxide thin films have been fabricated by e-beam evaporation,[16] reactive and rf sputtering,[17,18] thermal chemical vapor deposition (CVD),[19] and plasma-enhanced CVD[20] techniques. E-beam evaporation is a powerful technique used to prepare thin films at higher deposition rate and with controlled stoichiometry by adjusting the deposition parameters such as substrate temperature, oxygen pressure, and evaporation rate.[21,22] In this study, NiO/TiO films with various NiO film thicknesses were deposited by e-beam evaporation on glass and silicon substrates and then annealed at 500 °C in H_2 atmosphere for 1 h in order to obtained Ni nanograins with various sizes on the crystalline TiO film. The structure, morphology, ultraviolet–visible (UV–vis) transmittance, and visible light absorption were studied.

2. Experimental Procedure

The target materials of TiO_2 powder (ADMAT MIDAS, 99.99%) and NiO powder (Alfa Aesar, 99%) were formed and sintered at 1200 °C for 3 h. The substrates were cleaned with isopropyl alcohol (EPA) and deionized water (DI

*E-mail address: funs@mail.mse.ncku.edu.tw

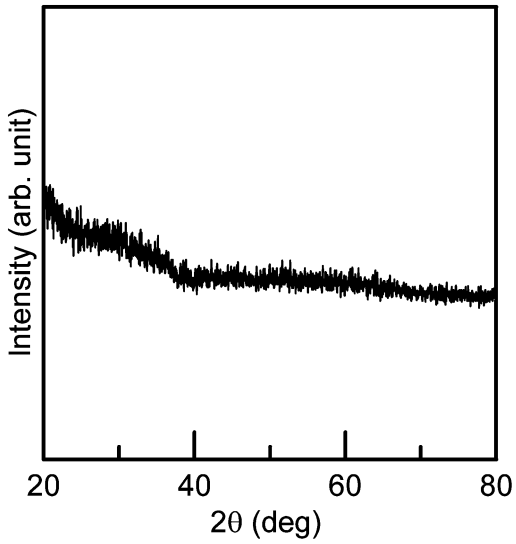

Fig. 1. XRD pattern of titanium oxide film deposited on silicon substrate at 200 °C.

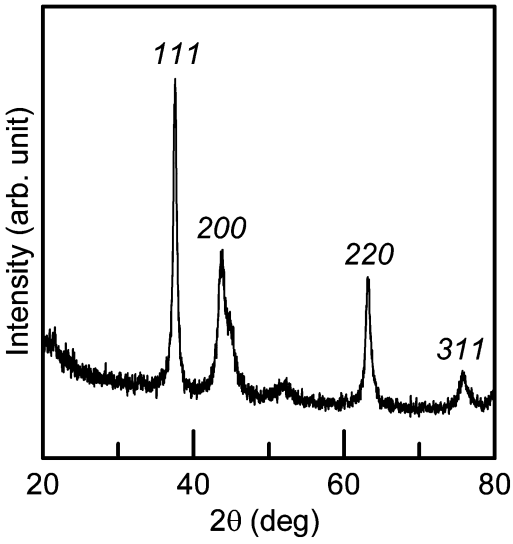

Fig. 2. XRD pattern of nickel oxide film deposited on titanium oxide at 200 °C.

water), and then dried under a flow of nitrogen gas. The substrate was fastened in a curved holder with a working distance of 20 cm and spun at a spin speed of 40 rpm. The substrates were heated using lamps to 200 °C. A diffusion-pumped vacuum system with a base pressure of 5×10^{-6} Torr was used for deposition. The deposition rate was controlled by e-beam power and monitored by a thickness control system (ULVAC CRTM-6000). TiO_2 thin films with a thickness of 500 nm were deposited on silicon and glass substrates by e-beam evaporation at 200 °C, and NiO thin films with thicknesses ranging from 10 to 320 nm were deposited on the TiO_2 film under the same deposition parameters. Then, the NiO films were annealed at 500 °C in H_2 atmosphere for 1 h under a heating rate of 10 °C/min.

The structures of NiO, TiO_2, and Ni/TiO_2 films were identified by X-ray diffraction (XRD) analysis with Cu Kα radiation and a Ni filter, operated at 30 kV, 30 mA, a scanning rate of 4°/min, and a 2θ in the range of 20–80° (Simens D5000). The morphology of the Ni/TiO_2 films was observed and analyzed by scanning probe microscopy (SPM; Seiko HV300). The optical transmittance and absorption levels of the Ni nanoparticle/TiO_2 thin film and glass substrate were measured by UV–vis spectrophotometry (HP Agilent 8453) at 190–1100 nm and (Hitachi U3010) at 200–800 nm.

3. Results and Discussion

A titanium oxide film was deposited on glass and silicon substrates by e-beam evaporation at 200 °C, and its structure was determined by XRD analysis, as shown in Fig. 1. The analysis revealed that the amorphous titanium oxide was obtained on both the silicon and glass substrates. For thin-film deposition, amorphous titanium oxide is usually obtained at low deposition temperatures. The mobility of the absorbed species is relatively low owing to the low substrate temperature, thus preventing these species from migrating to more energetic sites where nucleation can occur.[23] Amor *et al.*[24] reported that the amorphous titanium oxide film prepared by radio frequency magnetron sputtering was obtained at a lower temperature than 350 °C although high-energy ion bombardment was used in a sputtering process, and the unheated films are amorphous regardless of the sputtering parameters.[25] The color of the titanium oxide films prepared at room temperature was transparent, but a slight gray color was observed when deposited at 200 °C. Although the color of the thin film had changed, the structure of the titanium oxide was still amorphous, as shown in Fig. 1.

The NiO film was deposited on TiO_2/silicon or TiO_2/glass by e-beam evaporation and the structure was analyzed by XRD analysis, as shown in Fig. 2. In Fig. 2, the (111), (200), (220), and (311) reflections of the NiO thin film were obtained and the intensity ratio is close to the data of JCPDs card, which reveals that a polycrystalline NiO film with a random orientation was obtained. There was no preferred orientation, which is usually found in thin-film deposition processes.

NiO films were deposited on TiO_2/silicon or TiO_2/glass by e-beam evaporation at various thicknesses and then annealed at 500 °C in H_2 atmosphere for 1 h. The structure of the Ni/TiO_2 films determined by XRD analysis is shown in Fig. 3. Although titanium oxide exists in three different phases, namely, anatase, rutile, and brookite, only amorphous, anatase, and rutile films have been found for TiO_2 up to now.[26] The key factors influencing the microstructure of TiO_2 films are deposition temperature and annealing temperature.[24,27] At a low temperature, TiO_2 films with the anatase phase are more stable and change to the rutile phase at about 800 °C.[24] In Fig. 3, it was found that an anatase TiO_2 film was obtained, meanwhile, the diffraction peaks maintained nearly constant after being annealed at 500 °C. The structures of the crystalline TiO_2 films are the anatase phase with reflections of (101), (112), (200), and (204), as shown in Fig. 3. Battiston *et al.*[28] reported that thermal treatment at 500 °C in air for 3 h is not sufficient for inducing phase transformation to anatase and a transformation is observed only after 6 h of annealing in air at 500 °C. Such reluctance to crystallization is more marked in samples grown at low temperatures. In this study, the TiO_2 film was prepared by e-beam evaporation followed by annealing at 500 °C for 1 h,

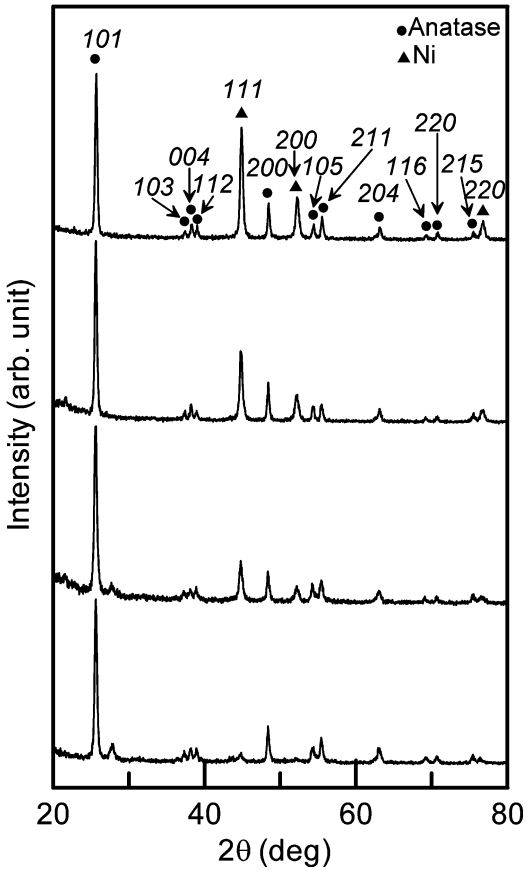

Fig. 3. XRD patterns of Ni/TiO_2 films reduced from NiO/TiO_2 films with NiO film thicknesses of (a) 10, (b) 40, (c) 80, and (d) 160 nm.

which is a shorter annealing time than that used by Battiston *et al.*[28] However, sharp diffraction peaks of the anatase phase were found in Fig. 3. For application as photocatalyst, the anatase phase has the highest photocatalytic activity[29] and is a good choice in that it provides an anticorrosion effect under UV illumination. Either the anatase or the rutile phase is usually observed in films prepared by PVD or CVD. In Fig. 3, we can also see that the intensity of the Ni diffraction peaks, i.e., (111), (200), and (220), increases as the thickness of the NiO film increases, which indicates that the particle size of Ni increased with the thickness of the NiO film increasing. Before the thickness of NiO film was higher than 80 nm, the Ni grains joined and began to form a thin film after annealing in H_2 atmosphere for 1 h. These samples with metallic color were observed and a very low resistivity was easily measured.

After annealing, Ni nanograins were reduced from the NiO film on the TiO_2 film. The surface morphologies of the Ni/TiO_2 films on the silicon substrates were observed by SPM, as shown in Fig. 4, and the influence of particle size was studied. In Fig. 4(a), isolated Ni nanograins formed, whose average size was less than 100 nm. It was found that the thicker NiO film, the larger the Ni particle. Furthermore, isolated grains coarsened and contacted each other resulting in island grain formation, and then a Ni film finally formed. In Fig. 4(c), a distinct morphology was found because of nickel film formation. From Fig. 4, it was demonstrated that the Ni nanograins on the TiO_2 film could be prepared by NiO film reduction and the average particle size of Ni could be decided by NiO film thickness.

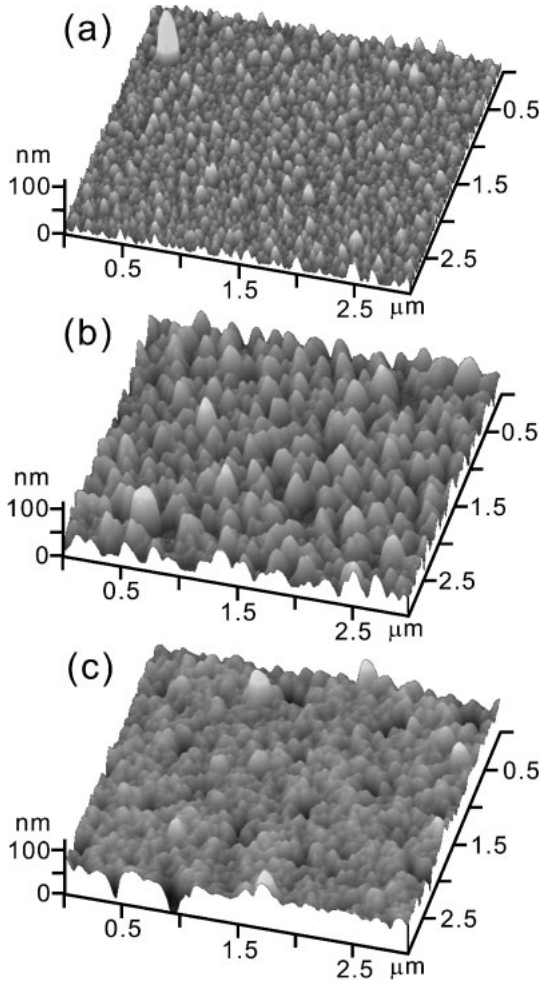

Fig. 4. SPM analysis of Ni/TiO_2 films reduced from NiO/TiO_2 films with NiO film thicknesses of (a) 10, (b) 40, and (c) 160 nm.

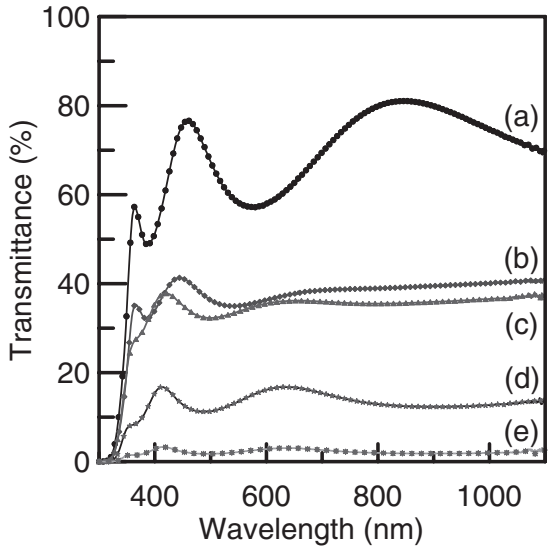

Fig. 5. UV–vis transmittance of Ni/TiO_2 films reduced from NiO/TiO_2 films with NiO film thicknesses of (a) 10, (b) 20, (c) 40, (d) 80, and (e) 160 nm.

Titanium oxide films are transparent in the visible region and its transparency exhibits a sharp decrease in the UV region.[30] The transmittance of the Ni–TiO_2 films is shown in Fig. 5, which shows that the transparent limitations are

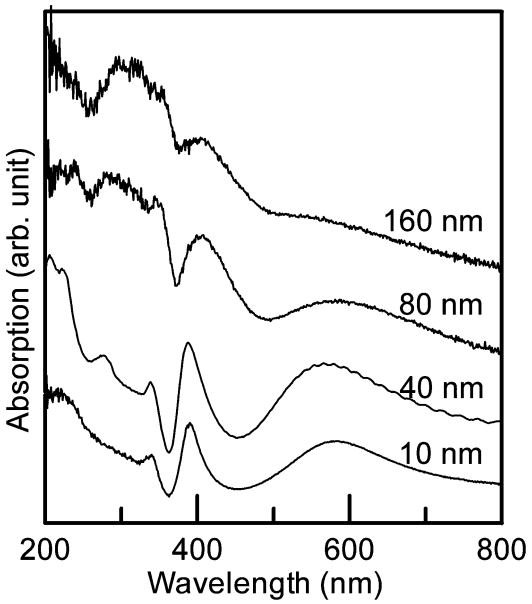

Fig. 6. Vis absorption levels of Ni/TiO_2 films reduced from NiO/TiO_2 films as function of NiO film thickness.

nearly constant because the TiO_2 films deposited in the same run were annealed at the same temperature of 500 °C. Martin *et al.*[31] reported similar results when TiO_2 films were annealed at a temperature lower than 700 °C, but the limitation shifted to a higher wavelength after annealing at 900 and 1100 °C. Hou and Choy[32] reported that the transparent limitation shifts to longer wavelength because of the rutile/anatase ratio of the films after various-temperature annealing. It can be observed that the shape of the spectra depends not only on the changes in nickel layer thickness, but also on changes in particle size. The transmittance decreased with an increase in Ni particle size, and a very low transmittance was found when the Ni film formed. In Fig. 5, a similar peak shape was found, but these peaks shift to a shorter wavelength with an increase in Ni nanoparticle size. At the same time, the transmittance decreased with an increase in Ni nanoparticle size, because the transparent area was occupied by Ni grains. Yoon *et al.*[33] reported that the visible-light absorption wavelength moves the shorter wavelength forward because the size of nanometallic particles decreased. According to our previous research, the highest transparent ratio of TiO_2 films on glass is higher than 90%; however, the lower transparent ratio was found because of Ni nanograins.

The vis absorption of Ni/TiO_2 films is showed in Fig. 6, which reveals the effect of Ni nanoparticle/TiO_2 film on the visible light absorption clearly. We found that the absorption peak shifts to longer wavelengths with Ni grain size increases.

4. Conclusions

Ni nanograins reduced on TiO_2 film can be prepared by depositing NiO/TiO_2 films using e-beam evaporation followed by annealing in H_2 atmosphere at 500 °C for 1 h. The Ni particle size increases with an increase in NiO film thickness, and grains coarsened and finally joined to form a thin film when the NiO film thickness is higher than 80 nm. For transmittance measurement, the peak shifts to a shorter wavelength and this trend was enhanced with a decrease in Ni particle size. For visible-light absorption measurement, the absorption peak shifted toward a longer wavelength with an increase in Ni particle size.

Acknowledgements

The financial support from the Nation Science Council, Taiwan, R.O.C. through a grant (No. NSC93-2216-E-2310-006) is greatly appreciated. The authors also sincerely thank Dr. S. J. Huang and Dr. C. H. Tai for their kind assistance in the transmittance measurements.

1) M. Takahashi, K. Mita, and H. Toyuki: J. Mater. Sci. **24** (1989) 243.
2) K. Ishibashi, Y. Nosaka, K. Hashimoto, and A. Fujishima: J. Phys. Chem. B **102** (1998) 2117.
3) C. Hobbs, R. Hegde, and B. Maiti: Symp. VLSI Technology Dig. Tech. Pap., 1999, p. 133J.
4) P. S. Peercy: Nature **406** (2000) 1023.
5) A. I. Kingon, J.-P. Maria, and S. K. Streiffer: Nature **406** (2000) 1032.
6) H. Sim, S. Jeon, and H. Hwang: Jpn. J. Appl. Phys. **40** (2001) 6803.
7) A. Fujishima, R. Wang, K. Hashimoto, T. Watanabe, M. Chikuni, E. Kojima, A. Kitamura, and M. Shimohigoshi: Adv. Mater. **10** (1998) 135.
8) A. Fujishima, T. N. Rao, and D. Tryk: J. Photochem. Photobiol. C **1** (2000) 1.
9) M. C. J. Bradford and M. A. Vannice: Appl. Catal. A **142** (1996) 73.
10) M. I. Litter: Appl. Catal. B **23** (1999) 89.
11) M. Anpo, M. Takeuchi, K. Ikeue, and S. Dohshi: Curr. Opin. Solid State Mater. Sci. **6** (2002) 381.
12) Q. G. Yan, W. Z. Weng, H. L. Wan, H. Toghiani, R. K. Toghiani, and C. U. Pittman, Jr.: Appl. Catal. A **239** (2003) 43.
13) M. A. Vannice and R. L. Garten: J. Catal. **56** (1979) 236.
14) D. Dissanayake, M. P. Rosynek, K. C. C. Kharas, and J. H. Lunsford: J. Catal. **132** (1991) 117.
15) C. T. Au and H. Y. Wang: J. Catal. **167** (1997) 337.
16) L.-J. Meng, M. Andritschky, and M. P. dos Santos: Thin Solid Films **223** (1993) 242.
17) M. Nakamura, T. Aoki, and Y. Hatanaka: Vacuum **59** (2000) 506.
18) M. Ivanda, S. Music, S. Popovic, and M. Gotic: J. Mol. Struct. **480–481** (1999) 645.
19) D. H. Lee, Y. S. Cho, T. S. Kim, J. K. Lee, and H. J. Jung: Appl. Phys. Lett. **66** (1995) 815.
20) Y. H. Lee, K. K. Chan, and M. J. Brady: J. Vac. Sci. Technol. A **13** (1995) 596.
21) K. Kawasaki, J. F. Despres, S. Kamei, M. Ishikawa, and O. Odawara: J. Mater. Chem. **7** (1997) 2117.
22) F. Zhang, X. Liu, Y. Mao, N. Huang, Y. Chen, Z. Zheng, Z. Zhou, A. Chen, and Z. Jiang: Surf. Coat. Technol. **103–104** (1998) 146.
23) X. Hou and K.-L. Choy: Surf. Coat. Tech. **180–181** (2004) 15.
24) S. B. Amor, L. Guedri, G. Baud, M. Jacquet, and M. Ghedira: Mater. Chem. Phys. **77** (2002) 903.
25) S. B. Amor, G. Baud, M. Jacquet, and N. Pichon: Surf. Coat. Technol. **102** (1998) 63.
26) P. Löbl, M. Huppertz, and D. Mergel: Thin Solid Films **251** (1994) 72.
27) Y.-Q. Hou, D.-M. Zhuang, G. Zhang, M. Zhao, and M.-S. Wu: Appl. Surf. Sci. **218** (2003) 98.
28) G. A. Battistona, U. R. Gerbasia, A. Gregoria, M. Porchiaa, S. Cattarinb, and G. A. Rizzic: Thin Solid Films **371** (2000) 126.
29) B. Ohtani, Y. Ogawa, and S. I. Nishimoto: J. Phys. Chem. B **101** (1997) 3746.
30) D. Mardare, M. Tasca, M. Delibas, and G. I. Rusu: Appl. Surf. Sci. **156** (2000) 200.
31) N. Martin, C. Rousselot, D. Rondot, F. Palmino, and R. Mercier: Thin Solid Films **300** (1997) 113.
32) X. Hou and K.-L. Choy: Surf. Coat. Technol. **180–181** (2004) 15.
33) J. W. Yoon, T. Sasaki, and N. Koshizaki: Electrochem. Solid-State Lett. **5** (2002) A256.